PROCEEDINGS OF SCIENCE

Study of K^0_S pair production in single-tag two-photon collisions at Belle

Sadaharu Uehara[*†]
KEK-IPNS, Institute for Particle and Nuclear Studies, High Energy Accelerator Research Organization, Tsukuba, Japan
E-mail: uehara@post.kek.jp

We report a measurement of the cross section for K^0_S pair production in single-tag two-photon collisions, $\gamma^*\gamma \to K^0_S K^0_S$, for Q^2 up to 30 GeV^2, where Q^2 is the negative of the invariant mass squared of the tagged photon. The measurement covers the kinematic range 1.0 GeV $< W <$ 2.6 GeV and $|\cos\theta^*| < 1.0$ for the total energy and kaon scattering angle, respectively, in the $\gamma^*\gamma$ center-of-mass system. These results are based on a data sample of 759 fb^{-1} collected with the Belle detector at the KEKB asymmetric-energy e^+e^- collider. For the first time, the transition form factor of the $f'_2(1525)$ meson is measured separately for the helicity-0, -1, and -2 components and compared with theoretical calculations. The $\gamma^*\gamma$ partial decay widths of the χ_{c0} and χ_{c2} charmonia are measured as a function of Q^2.

XXVI International Workshop on Deep-Inelastic Scattering and Related Subjects (DIS2018)
16-20 April 2018
Kobe, Japan

[*]Speaker.
[†]On behalf of the Belle Collaboration.

PoS(DIS2018)107

1. Introduction

With an e^+e^- collider, we can investigate various phenomena induced by two virtual or quasi-real photon collisions. Such reactions are useful to make tests of QCD through exclusive final-state processes, to measure resonance production and its properties, and to study for hadron spectroscopy and new resonance searches. Particularly, in the "single-tag" two-photon processes, where either photon is highly virtual and the other photon regarded as (quasi-) real, we can measure a Q^2 dependence of the transition form factor (TFF) of a meson which is produced by a formation process from two-photon fusion. The measurements of TFF or the $\gamma^*\gamma$ cross sections are applied for studies of QCD based on models of $q\bar{q}$ mesons [1] and exotic hadrons, and hadron tomography through an extraction of generalized distribution amplitude (GDA) [2]. In addition, the size of the cross sections can be a reference of the Light-by-Light hadronic contribution which is used in a theoretical evaluation of the muon's anomalous magnetic moment ($g-2|_\mu$) [3].

Experimentally, the single-tag two-photon processes are measured by the reaction $e^+e^- \to e(e) + \text{hadrons}$ at an e^+e^- collider, where (e) is not detected being scattered to extremely forward angles (Fig. 1a). It is possible to extract $\gamma^*\gamma$-incident-based cross section, $\sigma(W,Q^2)$, as a function of the two-photon center-of-mass (c.m.) energy W, and a virtuality of the high-Q^2 photon that is defined as the negative of its invariant mass ($Q^2 > 0$), with a factorization to two-photon luminosity function under Equivalent Photon Approximation. Particularly, in neutral-meson pair production processes of C-even eigenstate which we treat in this report, the bremsstrahlung diagram (of C-odd) is not mixed (Fig. 1b). In case of a single resonance formation, TFF of the resonance is proportional to the helicity amplitude of the production process. Thus, the squared sum of the TFF over the helicity states is proportional to the resonance production cross section, $\sum_\lambda |F_\lambda(Q^2)|^2 \propto \sigma(\gamma^*\gamma \to \text{Resonance})$, where λ is a helicity with respect to the direction of γ^* in the c.m. frame, and $F_\lambda(Q^2)$ is the TFF defined for each helicity state.

The measurements are performed using the Belle detector [4] at the asymmetric e^+e^- collider KEKB [5]. We use the collision data collected at e^+e^- c.m. energies near the $\Upsilon(4S)$ mass ($\sim$ 10.6 GeV) and the $\Upsilon(5S)$ mass ($\sim$ 10.9 GeV).

2. Previous measurements

Before discussing our latest measurement for the single-tag $K^0_S K^0_S$ production process, we briefly introduce our previous measurements on the $\pi^0\pi^0$ production [6, 7] and the zero-tag measurement of the $K^0_S K^0_S$ production [8] which are closely related to the present measurement. We have observed a scalar $f_0(980)$ resonance for the first time in the zero-tag $\gamma\gamma \to \pi^0\pi^0$ process, as a much smaller peak in the cross section spectrum compared with the huge peak from the tensor meson $f_2(1270)$ [6]. We have measured the same production process also with the single-tag mode, where one of the incident photon is highly virtual, and found that the $f_0(980)$ production is not much smaller comparing with the $f_2(1270)$ [7]. The results for TFFs for the $f_0(980)$ and $f_2(1270)$ have shown different steepness of Q^2 dependence among different spin and helicity states of these mesons. These natures are consistent with a prediction of the theory based on $q\bar{q}$-meson calculations [1].

With this context, the $K^0_S K^0_S$ process also attracts an interest of physics researchers. The process can explore the similar effects of another tensor meson dominated by the $s\bar{s}$ state, $f'_2(1525)$. In addition, an interference phenomenon between an f-meson ($I = 0$) and an a-meson ($I = 1$) is expected at the $K^0_S K^0_S$-mass threshold region ($\sim$ 1.0 GeV) and the tensor-meson mass region ($\sim$ 1.3 GeV). We have observed a cross-section peak at the mass of $f'_2(1525)$ and a destructive interference of the $f_2(1270)$ and $a_2(1320)$ mesons in the zero-tag mode [8]. However, we could not measure the cross section just at the mass threshold due to a lack of the trigger efficiency. Meanwhile an almost background-free (from a continuum production) signals from the even-parity charmonia, χ_{c0} and χ_{c2} have been obtained.

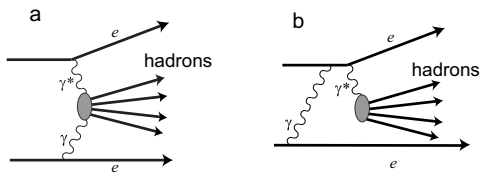

Figure 1: Feynman diagrams for (a) the single-tag two-photon process and (b) the bremsstrahlung (quasi-pseudo Compton scattering) process in e^+e^- collisions

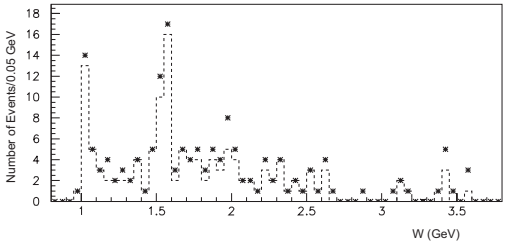

Figure 2: W distributions for the signal candidates for the $\gamma^*\gamma \to K^0_S K^0_S$ process, in the Q^2 region 3.0 GeV^2 (2.0 GeV^2)$< Q^2 <$ 30 GeV^2 for the dashed histogram (the asterisk plots).

3. Event selection for $\gamma^*\gamma \to K^0_S K^0_S$

Details of the analysis for the single-tag production of $K^0_S K^0_S$ state are shown in the published paper [9]. We cover the W region down to the mass threshold and up to the χ_{cJ} ($J = 0,2$) charmonia. There is no problem in the trigger efficiency thanks to relatively large transverse momenta of the tag electron and the final-state hadrons. We note that χ_{c1} does not decay to $K^0_S K^0_S$ due to symmetries of parity and identical bosons.

The final state for this analysis is $e^{\pm}(e^{\mp})K^0_S K^0_S$ with the K^0_S decaying to $\pi^+\pi^-$, where $(e^{\mp})$ is not detected. Thus the detected system consists of five tracks from one electron (or positron) and four charged pions. We require the electron candidate has a momentum $p > 1.0$ GeV/c and is identified as an electron by E/p, the ratio of the energy deposit on the electromagnetic calorimeter to the momentum measured by the central drift chamber. The charged pions are required to be separated from charged kaons with a loose cut using the particle-identification detectors. The neutral kaons are reconstructed from the $\pi^+\pi^-$ pair, where a finite decay flight length in the transverse plane to the beam axis and a two-dimensional selection criterion for the two K^0_S masses are required.

For the final candidates of the signal process, we apply a two-dimensional cut for the kinematical variables $E_{\rm ratio}$ and the p_t-balance. The $E_{\rm ratio}$ is the ratio of the measured to the expected energies of the $K^0_S K^0_S$ system in the e^+e^- c.m. frame, where the latter is calculated by the energy-momentum conservations of the whole reaction under the inputs of the measured invariant mass and scattering direction of the $K^0_S K^0_S$ system. An approximate p_t-balance in the e^+e^- c.m. frame

is required for the observed system, which implies that the missing $(e^{\mp})$ should have a very small p_t along the collision axis. We adopt a selection region of a half-elliptic shape centered at ($E_{\rm ratio}$, p_t-bal.)$= (1,0)$, in their two-dimensional plane.

From the reconstructed K^0_S mass and decay flight length distributions, we find that non-$K^0_S K^0_S$ backgrounds are negligibly small in the final candidates. Some backgrounds from the non-exclusive processes ($K^0_S K^0_S X$) are seen in the two-dimensional plot of the kinematical variables in the lowest W region below 1.3 GeV. We estimate a 14% background contamination in this region.

4. Derivation of the cross section and two-photon decay width

The obtained W distribution for the signal candidates (Fig. 2) shows the highest peak near the mass of $f'_2(1525)$, as the same as in the zero-tag measurement. In addition, we find an enhancement just above the $K^0_S K^0_S$ mass threshold (0.995 GeV), even taking the background contamination into account. Small peaks from the χ_{c0} and χ_{c2} charmonia are also seen.

Below $W < 2.6$ GeV, we derive the $\gamma^*\gamma$-based total cross section as a function of W for five Q^2 regions from 3 GeV^2 to 30 GeV^2 (Fig. 3). We assume the uniform c.m. angular distribution for the evaluation of the efficiency, and possible effect of different angular dependences are taken into account in the systematic uncertainty. The total systematic uncertainty is 13–24% dependent on W and Q^2 regions. We find the cross section has peaks near the threshold and the mass of $f'_2(1525)$. There is no significant enhancement in the $f_2(1270)/a_2(1320)$ region. The cross section gradually decreases according to Q^2.

Because the peaks from the two charmonium states are as narrow as the mass resolution of the detector, we evaluate the peak yields with the product of the two-photon decay width $\Gamma_{\gamma^*\gamma}$ and the branching fraction to the final state, instead of the W dependence of the cross section [9]. The experimental results are plotted as a function of Q^2 in Fig. 4 as a ratio to the corresponding zero-tag measurement (at $Q^2 = 0$) [8]. The Q^2 dependence is rather weak, and is consistent with the theoretical prediction [1] where the charmonium-mass scale is applied. A use of the ρ-mass scale does not match the data.

5. Partial-wave analysis for TFF of $f'_2(1525)$

We have performed a partial-wave analysis to obtain the TFF of $f'_2(1525)$. The angular differential cross section for the $\gamma^*\gamma \to K^0_S K^0_S$ process is decomposed to the contributions from the partial waves by extending it by spherical harmonic functions. We consider only the total spin $J = 0$ and 2 components ($J = 1$ is prohibited for $K^0_S K^0_S$, as mentioned above), and S and D_i are the introduced partial wave amplitudes for them, respectively, where $i = 0$, 1, 2 is the helicity of the spin-2 components.

The $f'_2(1525)$ resonance component is parametrized by the Breit-Wigner function for the W dependence, and its helicity fraction r_i is used to separate the contributions from the different helicities. Then, the TFF for the helicity λ is defined as $\sqrt{r_\lambda}|F_{f2p}(Q^2)|$. The experimental data have been fitted to obtain the TFF.

Due to problems from low statistics and mathematical non-deterministic nature, we parametrize W and Q^2 dependences of all the resonant and continuum components by empirical or known func-

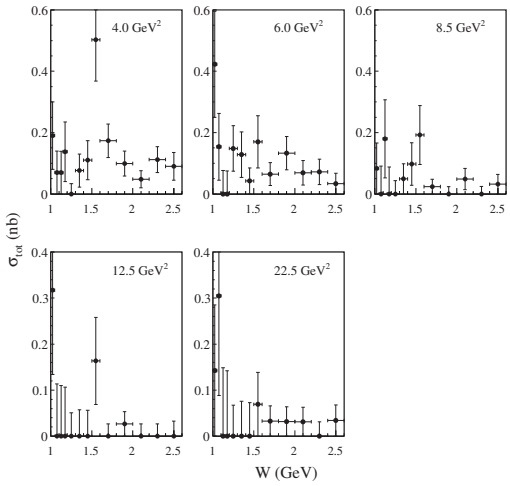

Figure 3: The $\gamma^*\gamma$-based total cross section for $\gamma\gamma^* \to K^0_S K^0_S$ as a function of W for the five Q^2 regions whose central value is shown in the subpanel.

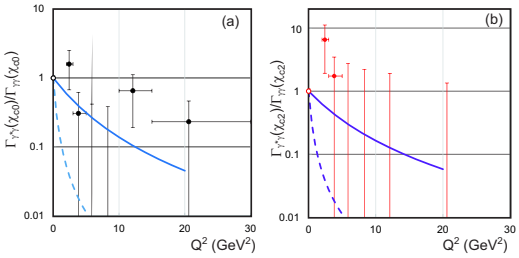

Figure 4: Q^2 dependence of the two-photon decay width of χ_{c0} (left) and χ_{c2} (right) normalized by that for $Q^2 = 0$. For the detailed definition and the curves, see the paper [9].

tions from previous studies. For example, we fix the interference and Q^2 dependence of the tensor mesons to assumptions inspired from the previous $\pi^0\pi^0$ measurement. Particularly, the helicity ratio for the $f_2'(1525)$ TFF is assumed to follow the following Q^2 dependences, $r_0 : r_1 : r_2 = k_0 Q^2 : k_1\sqrt{Q^2} : 1$, with the fraction parameters k_0 and k_1 left floated in the fit,

We need the angular differential cross section data for the partial-wave analysis. However, due to the low statistics, we cannot prepare them for the different Q^2 regions. Instead, we adopt a convention to use the Q^2-integrated experimental result of the angular distribution $N_{\rm EXP}(|\cos\theta^*|, |\phi^*|)$ corrected by the angular dependence of the acceptance, as the normalized differential cross section. We regard it as the angular dependence at $Q^2 = 6.5$ GeV^2, after the average value of Q^2 for the experimental samples.

The obtained Q^2 dependences of the $f_2'(1525)$ TFFs are plotted in Fig. 5. The curves are the theoretical prediction [1]. They show good agreement for the helicity-0 and 2 states. As for the helicity-1, the prediction is slightly larger, but is not inconsistent.

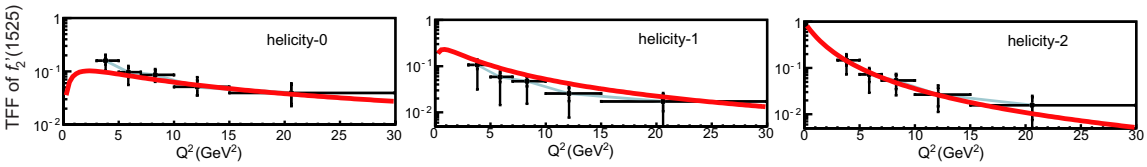

Figure 5: TFFs for the three helicity states of the $f_2'(1525)$ from the present measurement. The gray band shows the normalization error. The curves are from a theoretical prediction [1]

.

6. Threshold enhancement

We find a significant enhancement of the cross section at the lowest W bin below 1.05 GeV, compared with that in the two adjacent higher-W bins for 1.05 – 1.15 GeV. The Q^2 dependence is compared with the theoretical model [1] assuming that this follows that of a meson resonance. The experimental statistics are poor, and they are not inconsistent to each other.

7. Summary

We have measured the cross section of K^0_S pair production in the single-tag two-photon process, $\gamma^*\gamma \to K^0_S K^0_S$ up to $Q^2 = 30$ GeV^2 based on a data sample of 759 fb^{-1} collected with the Belle detector at the KEKB asymmetric-energy e^+e^- collider [9]. The data cover the kinematic ranges 1.0 GeV $< W <$ 2.6 GeV, $|\cos\theta^*| < 1.0$, and $0 \leq |\varphi^*| \leq 180^\circ$ in the $\gamma^*\gamma$ c.m. system. For the first time, we find production of the $f_2'(1525)$, $\chi_{c0}(1P)$, and $\chi_{c2}(1P)$ mesons in high-Q^2 $\gamma^*\gamma$ scattering. These resonances are most visible in the corresponding no-tag mode [8]. We have measured the χ_{c0} and χ_{c2} partial decay widths $\Gamma_{\gamma^*\gamma}$ as a function of Q^2. A partial-wave analysis has been conducted, and the helicity-0, -1, and -2 transition form factors (TFFs) of the $f_2'(1525)$ meson are measured. We have measured the total cross section near the $K^0_S K^0_S$ mass threshold.

The Q^2 dependence of the above resonances and structures are compared with the $q\bar{q}$-meson model predictions [1], and the comparisons show that they are not inconsistent for all of them.

References

[1] G. A. Schuler, F. A. Berends, and R. van Gulik, Nucl. Phys. B **523**, 423 (1998).

[2] S. Kumano, Qin-Tao Song, and O.V. Teryaev, Phys. Rev. D **97**, 014020 (2018).

[3] G. Colangelo, M. Hoferichter, B. Kubis, M. Procura and P. Stoffer, Phys. Lett. B **738**, 6 (2014).

[4] J. Brodzicka *et al.* (Belle Collaboration), Prog. Theor. Exp. Phys. **2012**, 04D001 (2012).

[5] T. Abe *et al.*, Prog. Theor. Exp. Phys. **2013**, 03A003 (2013).

[6] S. Uehara *et al.* (Belle collaboration), Phys. Rev. D **78**, 052004 (2008); S. Uehara *et al.* (Belle collaboration), Phys. Rev. D **79**, 052009 (2009).

[7] M. Masuda *et al.* (Belle Collaboration), Phys. Rev. D **93**, 032003 (2016).

[8] S. Uehara *et al.* (Belle Collaboration), Prog. Theor. Exp. Phys. **2013**, 123C01 (2013).

[9] M. Masuda *et al.* (Belle Collaboration), Phys. Rev. D **97**, 052003 (2018).

PoS(DIS2018)107